# Damage assessment in CFRP laminates exposed to impact fatigue loading

**George Tsigkourakos[1*], Vadim V Silberschmidt and I A Ashcroft**

Wolfson School of Mechanical and Manufacturing Engineering, Loughborough University, Leicester-shire, LE11 3TU, UK

* Corresponding author: Ashby Road, Loughborough, Leics., LE11 3TU, UK. Phone: +44-1509-227504. Fax: +44-1509-227502. E-mail: G.Tsigkourakos@lboro.ac.uk

**Abstract.** Demand for advanced engineering composites in the aerospace industry is increasing continuously. Lately, carbon fibre reinforced polymers (CFRPs) became one of the most important structural materials in the industry due to a combination of characteristics such as: excellent stiffness, high strength-to-weight ratio, and ease of manufacture according to application. In service, aerospace composite components and structures are exposed to various transient loads, some of which can propagate in them as cyclic impacts. A typical example is an effect of the wind gusts during flight.

This type of loading is known as impact fatigue (IF); it is a repetition of low-energy impacts. Such loads can cause various types of damage in composites: fibre breaking, transverse matrix cracking, de-bonding between fibres and matrix and delamination resulting in reduction of residual stiffness and loss of functionality. Furthermore, this damage is often sub-surface, which reinforces the need for more regular inspection.

The effects of IF are of major importance due its detrimental effect on the structural integrity of components that can be generated after relatively few impacts at low force levels compared to those in a standard fatigue regime. This study utilises an innovative testing system with the capability of subjecting specimens to a series of repetitive impacts. The primary subject of this paper is to assess the damaging effect of IF on the behaviour of drilled CFRP specimens, exposed to such loading. A detailed damage analysis is implemented utilising an X-ray micro computed tomography system. The main findings suggested that at early stages of life damage is governed by o degree splits along the length of the specimens resulting in a 20% reduction of stiffness. The final failure damage scenario indicated that transverse crasks in the 90 degree plies are the main reason for complete delamination which can be translated to a 50% stiffness reduction.

**Key words**: Impact fatigue, micro CT; CFRP; cracks

## 1. Introduction

The use of carbon fibre reinforced polymers (CFRPs) in the aerospace and other high technology industries has increased enormously in the last few decades and looks set for significant further expansion. This has been largely because of the high specific stiffness and strength i of these materials. However, other properties such as fatigue resistance, property tailoring and manufacturing flexibility are also of significance in certain applications.

CFRP structures in aerospace, and other, structural applications are generally subjected to some form of cycling loading, i.e. fatigue. In the laboratory, fatigue is generally approximated as a sinusoidally varying load or stress, characterised by the load ratio, frequency and maximum force. This type of loading can be termed standard fatigue (SF). However, real-life loading histories often involve vibrating loads that can propagate in structural elements as cyclic impacts. This phenomenon is known as impact fatigue (IF) [1]. IF is of major importance to the structural integrity of components and structures due to its detrimental effect on performance, which can occur after a relatively small number of low amplitude cycles [1-2].

Fatigue loading can cause various types of damage in laminate composites; eg. fibre breakage, transverse matrix cracking, de-bonding between fibres and matrix and delamination, resulting in a reduction of the residual stiffness and a loss of functionality [3-5]. More specifically, although CFRPs can carry large in-plane loads they have poor transverse properties, especially when subjected to low velocity impacts, which has an impact on the in plane strength as well. Such events can take place without leaving evidence of the damage on the surface of the component, therefore, non-destructive techniques (NDT), such as X-ray micro-computer tomography (MCT), are required for characterisation of internal flaws. X-ray MCT has been applied to date, mostly to metal-matrix and ceramic-matrix composites under drop-weight tests [6-12]. Some work has been carried with polymer matrix composites to characterise impact damage; investigating the fibre fracture and delamination associated with penetration tests [13-16]. The purpose of the current study is to utilise the capabilities of X-ray micro-CT for the characterization of impact damage induced by the uniaxial tensile testing of CFRP and also investigate any stiffness reduction associated with the observed damage.

## 2. Experimental details

### 2.1 Material samples

Composite samples were made using unidirectional carbon/epoxy T700/LTM45 prepreg with a nominal ply thickness of 0.128 mm. The T700 fibre is used in the wings and the fuselage of airplanes and is due to its high strength. LTM45 is a toughened , low temperature curing epoxy resin capable of high temperature end use. The composite system T700/LTM45 (From Advanced composite Group), was mainly selected because it can be easily cured at low temperature and its mechanical property database is available in Loughborough University. Its UD mechanical properties were measured as $E_1$ of 127GPa, $E_2$ of 9.1GPa, $G_{12}$ of 5.6GPa and $v_{12}$ of 0.31.

A symmetric cross-ply lay-up of $0_2/90_4/0_2$ was selected, as this enables a number of failure mechanisms to be investigated in a relatively simple system. .Laminates of 100 × 150 mm were laid up in an 8-ply stacking arrangement and cured in an autoclave at 60°C under a pressure of 0.62 MPa (90 psi) for 18 hours. The thickness of the cured plate was approximately 1mm. Each sandwich panel was then cut into four 25 mm × 150 mm specimens.

2.2 Specimen preparation

The specimen configuration, as shown in figure 1, was adopted in conformity with BS EN ISO8256:2004, with modification to fit the tensile impact machine figure 3. End tabs were used to aid grip and provide sample alignment. These were made of aluminium alloy and bonded to the specimens with FM-73 adhesive. Holes were drilled in the specimens using a diamond coated 6 mm drill specially designed to attenuate delamination. The hole at the left end of the sample in figure 2 was used to attach the sample to the specimen support via a bolt. The hole in the centre of the sample was introduced as a representation of a bolt hole and to provide region to initiate damage.

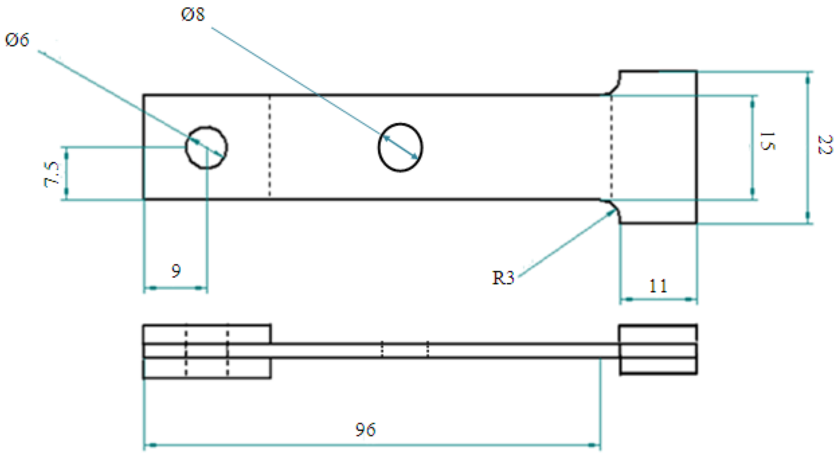


**Figure 1.** Dimensions of the specimens in mm.

2.3 Uniaxial tensile impact test

The tensile impact test used for our experiments utilises a CEAST RESIL impactor. The basis of this method is that a specimen is supported at one end in a vice and its opposite end is struck repeatedly by a controlled pendulum hammer, resulting in a dynamic uniaxial tensile load as shown in figure 2. The specimen is clamped at one end to a specimen support using bolts. A load cells also rigidly fixed to this support. At the free end of the specimen an  special impact block is fixed. This block consists of a two plates held together by bolts. A firm connection between the specimen and impact block is obtained by compression of the plates. The impact block is struck by a pendulum hammer at the location indicated in Figure 2(a).

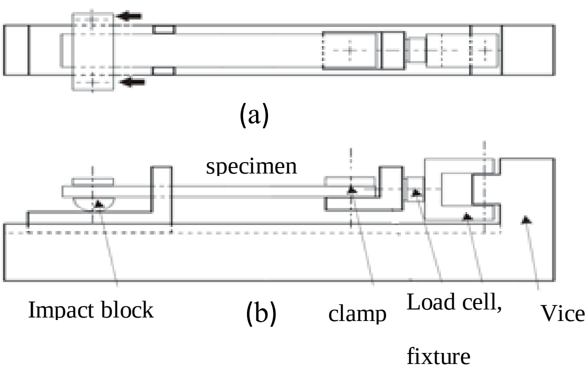


**Figure 2.** Schematic of specimen fixture for impact fatigue. (a) Top view, arrows denote impact loading direction. (b) Side view.

The pendulum hammer is released from a pre-selected initial angle in the range of 0-150° which corresponds to a potential energy in the range of 0-4 J and velocity between 0-3.7 m/s. The impact of the pendulum hammer produces a tensile load in the specimen over a period of 6-7 ms. The period between the impacts is approximately 15 s. The evolution of force during each impact can be monitored for 5 µs with up to 8000 data points for each impact. The amplified and filtered data are then downloaded to a computer as magnitudes of force and time and this data is then used to calculate velocity *V*, displacement, *d*, and energy, *E*, for each impact. The specimens were impacted at 1J which corresponds to a hammer velocity of 1.48m/s. They were subjected to 10, 600, 900 and 1200 impacts and up to failure. Force and stiffness data were acquired at every stage and damage was characterised using X-ray micro-CT.

2.4 X-Ray microtomography.

X-ray micro-CT measurements were performed using an XT H 225 X-ray and CT inspection system supplied from Nikon metrology instruments**.** The system consists of a 1-dimensional x-ray detector that captures the 2-dimensional cross-sections of the object projected from an electronic x-ray source. The source is a sealed X-ray tube operating at 25–225 kV with a 3 µm spotsize. Data were collected at 50 kV and 80 µA. An object manipulator with two translations and one rotation facilitates rotating the sample for acquisition of tomographic data, raising/lowering the sample to select a region of interest, and translating along the optical axis to adjust the magnification. For 3-D reconstruction, transmission X-ray images were acquired from 3600 rotation views over 360° of rotation (0.1° rotation step). Following acquisition, a software program builds a 3D volume dataset by 'stacking' the individual slices one on top of the other.

**3. IF test results**

Impact tests were conducted with a constant applied energy, this means that the applied force is not a controllable variable as it is affected by the deterioration of the specimen as a result of fatigue. Typical graphs showing the evolution of the force response to impacts at various stages in a sample's life are presented in figure 3. *F*(*t*) is the force response as a function of time, t, and $F_{0max}$ is the maximum force obtained in the initial impact. Damage is identified as a deterioration of $F_{max}$ under continuing impact cycles and a drastic change is seen in the final breaking impact (ultimate life).

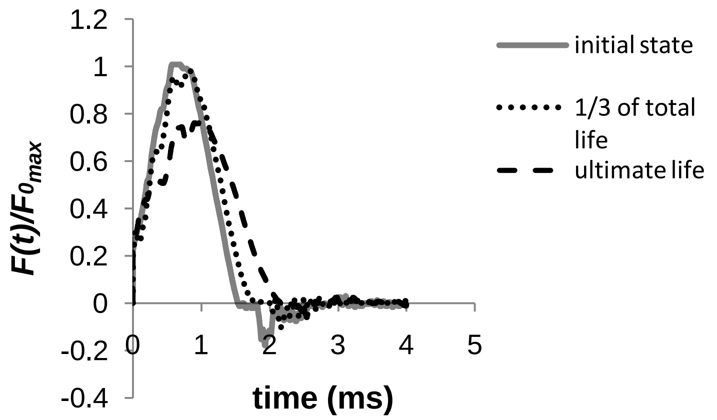


**Figure 3.** Evolution of forces in specimen in various cycles of impact fatigue.

The reduction in $F_{max}$ with increasing number of impacts can be seen in figure 4. This is accompanied with a reduction in stiffness, as shown in figure 5.These two figures indicate that the studied response is changing as a function of damage accumulated in the sample as a result of the repeated impacts.

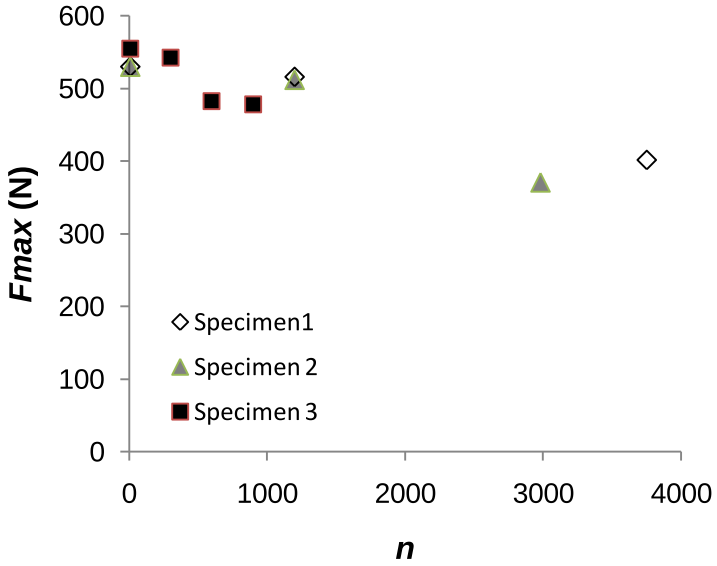


**Figure 4.** Deterioration of *Fmax* as a function of number of cycles.

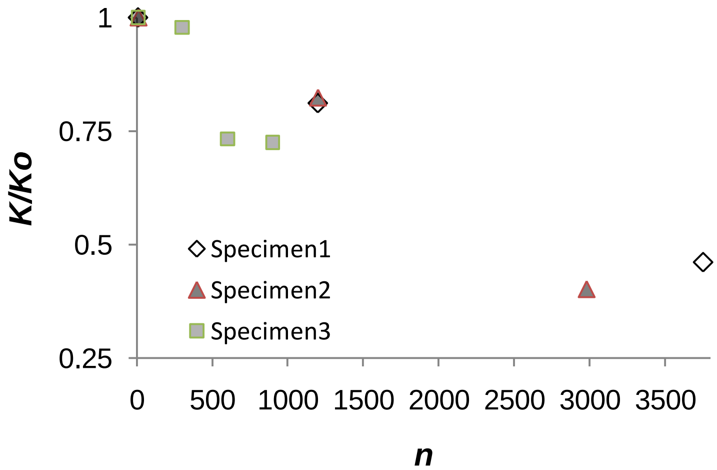


**Figure 5.** Deterioration of *K* with respect to number of cycles

From the above figure it is apparent that the decrease in stiffness after 40% of life is drastic. The preliminary objective of the paper is to correlate the changes in stiffness and force with the observed damage in the sample. This will be described in the following section.

## 4. Macroscopic and microscopic evaluation of damage

Macroscopic evaluation at early stages of the fatigue life of the samples revealed only 0º cracks in the outer plies of the samples. For that reason microscopic evaluation utilising Xrays was performed. Figure 6 shows the inspection area as well as the sectioning procedure of the post processing of the results. The individual slices that were examined along the x and y axes revealed that the maximum damage was located at the edges of the hole were the stress concentrations were high. A symmetric pattern of damage was observed on either side of the hole in both the x and y directions. For this reason slices y1 and x3 were selected for comparison of damage patterns after 300 900 and 1200 impacts.

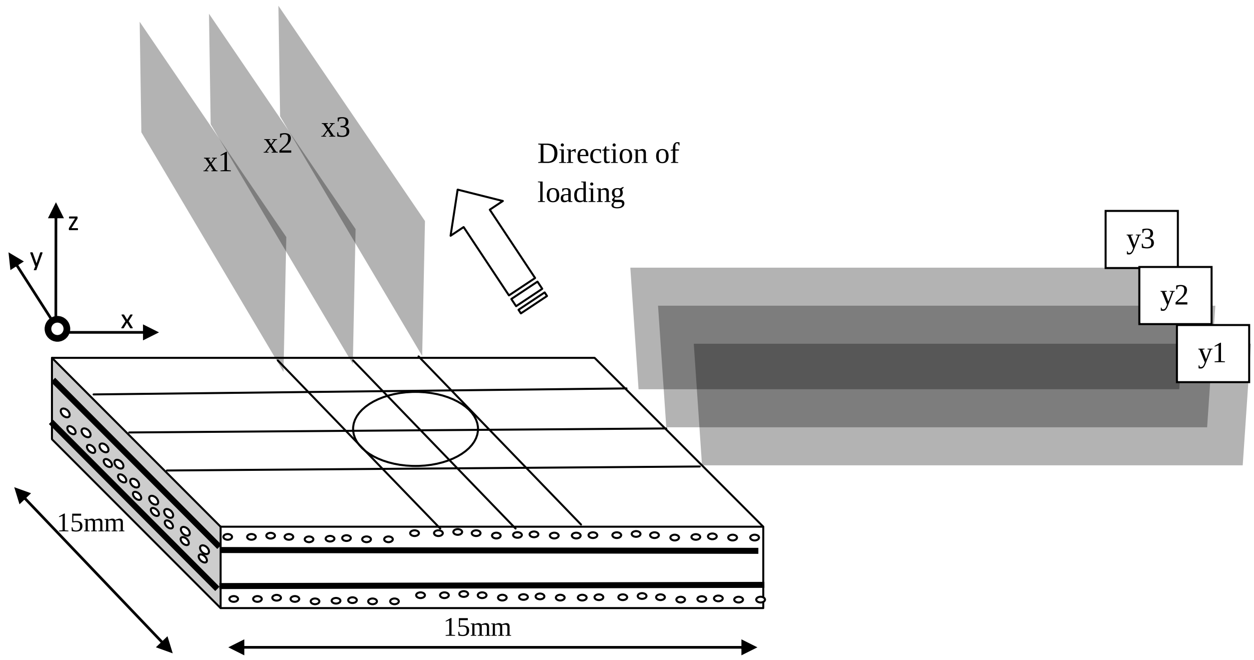


**Figure 6.** Schemating indicating the postprocessing procedure and direction of loading. Slices selected at the edges and centre of the hole along the x and y axes .

Figure 7 presents the slices along the y axis while figure 8 along the x axis. In figure 7 is it is apparent that the axial cracks initiated by microdefects at the virgin state figure 7(a) are evolving by increasing in width and length as they reach the 90 degree plies figure 7(b)-(d). At the final stage of damage Figure7 (e) these axial cracks are joined by delamination and complete decohesion of the 0 degree plies takes place. In Figure 8 the slices along the x axis are demonstrated. Delamination signs are vivid at the area adjacent to the hole and seem to grow away from the hole along the length of the specimen. Transverse cracks in the 90 degree plies grow towards the 0/90 and 90/0 interfaces joining the delaminations at areas next to the drilled area. Finally 3D views of the last stage of damage show the complete failure scenario in figure 9.

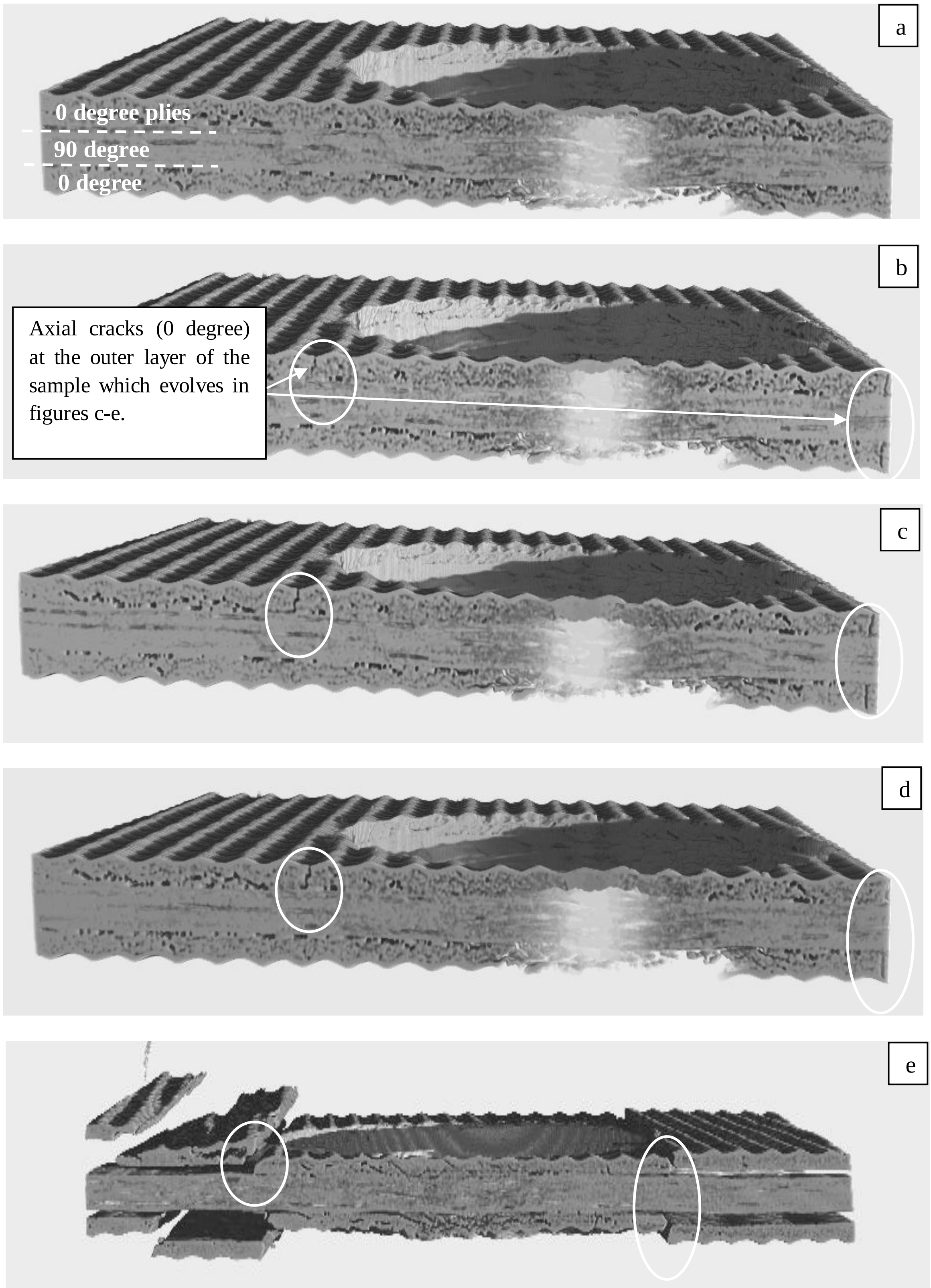


Figure 7. Individual y1 slices at a) post-manufacturing state, b) 300 impacts , c) 900 impacts ,d)1200 impacts and e) 3750 impacts(ultimate life)

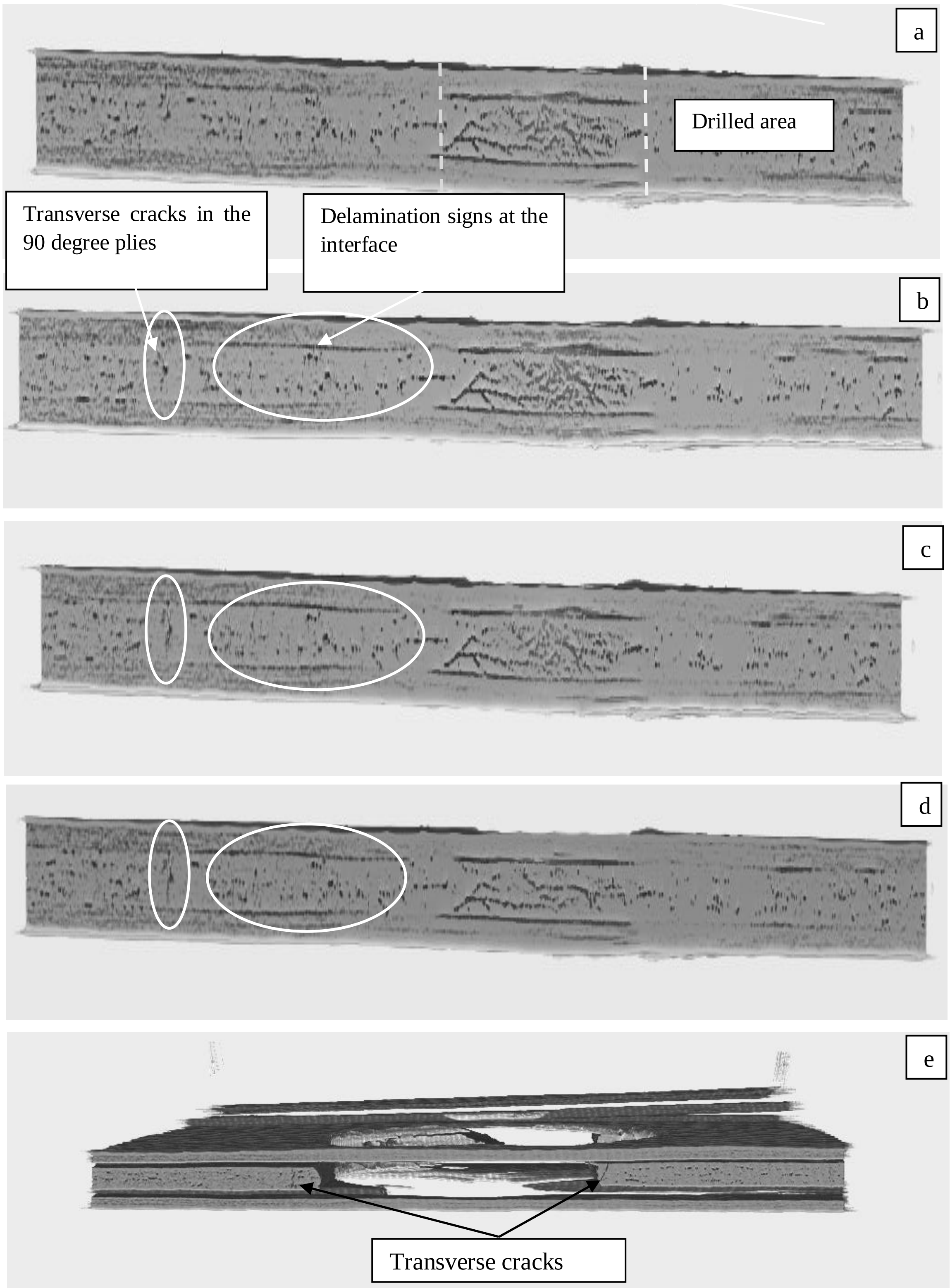


Figure 8. Individual x3 slices at a) post-manufacturing state, b) 300 impacts , c)900 impacts ,d)1200 impacts and e)3750 impacts(ultimate life)

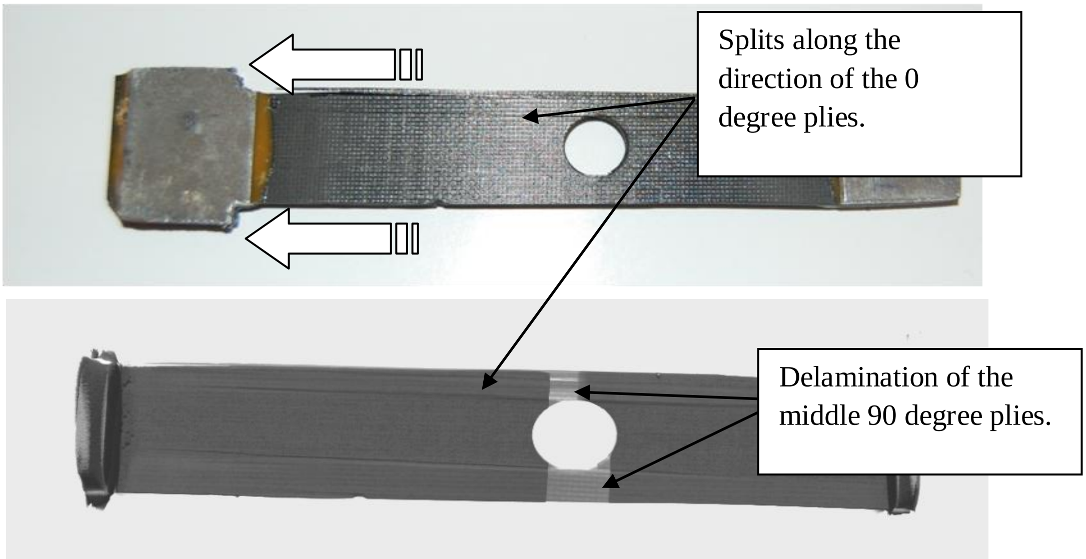


**Figure 9.** (a)Macroscopic evaluation with arrows denoting the direction of loading, (b) Semitransparent Xray front view of the whole specimen at the final stage of damage.

**5. Results and discussion**

In this paper a qualitative analysis on the effect of IF in damage propagation was carried out by means of Xray-micro Ct. Results showed that in crossply laminates a 20% decrease in stiffness can be reasoned by the growth of already existing microcracks/defects. More specifically 0 degree splits in the direction of the loading that propagated towards the 0/90 and 90/0 interface as shown in Figure 7.It has to be noted that the length of these cracks was also increased along to the length of the specimen and adjacent to the hole edges in the direction of the loading until the whole specimen was governed by them as shown figure 10.These 0 degree splits created an increase in the distance between the 0 and 90 plies in figures 8b,c . This seems that initiated delamination that was reinforced by transverse cracks in the 90 degree plies figures 8b-d. The 20% stiffness decrease occurs at very early stages of impact life (30-40%) and it was very small compared to the 50% decrease at the final stages of failure. The final stages of failure revealed a complete delamination pattern with 0 degree splits along the length of the specimen. More experimentation is required for damage states between 1/3 and the total impact life to reveal the exact damage progression scenarios. However based on the results the transverse crack formation seems to be the foundation for this major stiffness reduction since delamination was augmented after the 1/3 of life. this paper sets the foundation for a stiffness model applicable to IF regime and is a starting point for quantifying damage at various stages of life by measuring the defective volume, delamination area and contrast it with the reduction in stiffness.

**6. Conclusions**

Significant stiffness decrease occurs at late stages of impact life in crossply laminates and is governed by delaminations caused by tranverse cracks and 0 degree splits. At the initial stages of life 0 degree splits are the predominant failure mechanism and can be related to a 20% stifness reduction. The fact that a 50 % reduction of stiffness occurred when the 90 degree plies failed completely shows that although composites can carry large in-plane loads their mechanical properties can be seriously altered especially when they are subjected to low velocity impacts.

**References:**


[1] J P Casas-Rodriguez, I A Ashcroft and V V Silberschmidt, Damage evolution in adhesive joints subjected to impact fatigue, *J. Sound Vib* **308** (2007) 467-478.

[2] J P Casas-Rodriquez, I A Ashcroft and V V Silberschmidt, Damage in adhesively bonded CFRP joints: sinusoidal and impact fatigue , *Comp Sci Tech*, 2008,**68**,pp.2663-2670.

[3] I A Ashcroft , J P Casas-Rodriguez and V V Silberschmidt, Mixed mode crack growth in bonded composite joints under standard and impact fatigue loading, *J. Mat. Sci*., 2008, **43**, pp. 6704-6713.

[4] T Sınmazçelik , A A Arıcı and V Günay ,Impact–fatigue behaviour of unidirectional carbon fibre reinforced polyetherimide (PEI) composites, *Mater Sci*,2006,**41** pp.6237-6244.

[5] MÖ Bora, O Çoban O, T Sinmazçelik , I Cürgül, V Günay, On the life time prediction of repeatedly impacted thermoplastic matrix composites. *Materials & Design*, 2009,**30**, pp.145-153.

[6] E Maire, L Babout, J Y Buffiere and R Fougeres, Recent results on 3D characterisation of microstructure and damage of metal–matrix composites and a metallic foam using x-ray tomography, *Mat Sci Eng A – Struct* 2001, **319** , pp. 216–219.

[7] S A Mcdonald, M Preuss, E Maire, J Y Buffiere, P M Mummery and P J Withers, X-ray tomographic imaging of Ti/SiC composites, J *Micros – Oxford* , 2003, **209** (Part 2), pp. 102–112.

[8] P M Mummery, B Derby, P Anderson, G R. Davis and J C Elliot, X-ray mictrotomographic studies of metal–matrix composites using laboratory X-ray sources, *J Micros*,1995 ,**177**, pp. 399–406.

[9] A Borbély, H Biermann, O Hartmann and J Y Buffiere, The influence of the free surface on the fracture of alumina particles in an Al–Al2O3 metal–matrix composite, *Comp Mater Sci* , 2003, **26**, pp. 183–188.

[10] L Babout, W Ludwig, E Maire and J Y Buffiere, Damage assessment in metallic structural materials using high resolution synchrotron X-ray tomography, *Nucl Instrum Meth B* 2003,**200**, pp. 303–307.

[11] I Justice, P Anderson, G Davis, B Derby and J Elliot, Damage nucleation and growth in particle rein-forced aluminium matrix composites, *Key Eng Mat*, 1997, **127–131**, pp. 945–952.

[12] G Geandier, A Hazotte, S Denis, A. Mocellin and E Maire, Microstructural analysis of alumina chromium composites by X-ray tomography and 3-D finite element simulation of thermal stresses, *Scripta Mater* 2003 ,**48**, pp. 1219–1224.

[13] O Çoban O, MÖ Bora, T Sinmazçelik, I Cürgül, V Günay. Fracture morphology and deformation characteristics of repeatedly impacted thermoplastic matrix composites. *Materials & Design* , 2009, **30**, pp. 628-634.

[14] D D Symons, Characterisation of indentation damage in 0/90 lay-up T300/914 CFRP, *Compos Sci Technol* 2000, **60**, pp. 391–401.

[15] J P Dunkers, D P Sanders, D L Hunston, M J Everett and W H Green, Comparison of optical coherence tomography, X-ray computed tomography, and confocal microscopy results from an impact damaged epoxy/E-glass composite, *J Adhesion* 2002 , **78**, pp. 129–154.

[16] R H Bossi and G E Georgeson, Composite structure development decisions using X-ray CT measurements, *Mater Eval*, 1995, pp. 1198–1203.